Title

Impact on in-depth immunophenotyping of delay to peripheral blood processing.

Journal

Clinical & Experimental Immunology, 217(2)

Authors

Higdon, Lauren
Scheiding, Sheila
Kus, Anna
et al.

Publication Date

2024-07-12

DOI

10.1093/cei/uxae041

Peer reviewed

Clinical and Experimental Immunology, 2024, **217**, 119–132
https://doi.org/10.1093/cei/uxae041
Advance access publication 2 May 2024
Research Article

Clinical & Experimental IMMUNOLOGY

OXFORD

Research Article

Impact on in-depth immunophenotyping of delay to peripheral blood processing

Lauren E. Higdon[1], Sheila Scheiding[2], Anna M. Kus[2], Noha Lim[1], S. Alice Long[2], Mark S. Anderson[1] and Alice E. Wiedeman[2,*]

[1]Biomarker and Discovery Research, Immune Tolerance Network, San Francisco, CA, USA
[2]Center for Translational Immunology, Benaroya Research Institute, Seattle, WA, USA

[*]Correspondence: Alice Wiedeman, Center for Translational Immunology, Benaroya Research Institute, Seattle, WA, USA.
Email: awiedeman@benaroyaresearch.org

Abstract

Peripheral blood mononuclear cell (PBMC) immunophenotyping is crucial in tracking activation, disease state, and response to therapy in human subjects. Many studies require the shipping of blood from clinical sites to a laboratory for processing to PBMC, which can lead to delays that impact sample quality. We used an extensive cytometry by time-of-flight (CyTOF) immunophenotyping panel to analyze the impacts of delays to processing and distinct storage conditions on cell composition and quality of PBMC from seven adults across a range of ages, including two with rheumatoid arthritis. Two or more days of delay to processing resulted in extensive red blood cell contamination and increased variability of cell counts. While total memory and naïve B- and T-cell populations were maintained, 4-day delays reduced the frequencies of monocytes. Variation across all immune subsets increased with delays of up to 7 days in processing. Unbiased clustering analysis to define more granular subsets confirmed changes in PBMC composition, including decreases of classical and non-classical monocytes, basophils, plasmacytoid dendritic cells, and follicular helper T cells, with each subset impacted at a distinct time of delay. Expression of activation markers and chemokine receptors changed by Day 2, with differential impacts across subsets and markers. Our data support existing recommendations to process PBMC within 36 h of collection but provide guidance on appropriate immunophenotyping experiments with longer delays.

Keywords: peripheral blood mononuclear cells, immunophenotyping, CyTOF, delayed processing, monocytes

Abbreviations: cDC: conventional dendritic cell; CyTOF: cytometry by time-of-flight; DC: dendritic cell; DMSO: dimethylsulfoxide; K2 EDTA: dipotassium ethylenediaminetetraacetic acid; DISCOV-R: distribution analysis across clusters of a parent population overlaid with a rare subpopulation; DN: double negative T cells; Tfh: follicular helper T cell; HA: healthy adult; Hep: heparin; HuAB: human AB serum; MAIT: mucosal-associated invariant T; NK: natural killer; PBMC: peripheral blood mononuclear cell; PBS: phosphate-buffered saline; pDC: plasmacytoid dendritic cell; RBC: red blood cell; Treg: regulatory T cell; RA: rheumatoid arthritis; Th: T helper; UMAP: uniform manifold approximation and projection.

Introduction

Immune cell profiling of blood samples is an important approach for research on immune-mediated disease. This research can include the biology of the disease, the effects or mechanism of action of therapy or treatment, and the discovery or monitoring of prognostic or predictive biomarkers. Peripheral blood mononuclear cells (PBMC), which represent diverse white blood cells including lymphocytes and monocytes, are typically isolated from whole blood prior to immune cell profiling using a density gradient [1, 2]. The isolation of PBMC allows for cryopreservation and indefinite storage of samples for evaluation in batches and at a later time.

Isolation of PBMC requires specialized training, reagents, and equipment. For multicenter studies including clinical trials, the blood samples are often transported to a central laboratory that has facilities for further processing and storage to ensure consistency in processing across samples. Owing to the logistical practicalities of transporting from the site of blood sample collection to the PBMC processing laboratory, there is commonly a delay of at least a day between blood collection and PBMC processing.

Delays in blood processing can have effects on immune cell quality and composition. PBMC yield and viability generally decline as the processing delay increases, with small decreases seen by 24 h but significant drops after 2 days [3–18]. Granulocyte contamination increases within 24 h, which can differentially affect the integrity of other cell subsets [3, 12–14, 18–22]. Moreover, storage in extreme temperatures (< 10°C or > 37°C) increases granulocyte contamination and reduces PBMC yield [8, 13, 20].

Immune profiling demonstrates that within 24 h, there is typically a significant loss of monocyte subsets, natural killer (NK) cells, and regulatory T cells. In contrast, total B and T cells remain stable, though subsets thereof or marker expression may vary [4–6, 9, 10, 12–15, 19, 22, 23]. Few studies have reported immune cell composition in samples beyond a delay of 24 h, but those studies indicate the same trends [4, 5, 10]. While overall these studies demonstrate that processing delays have impacts across immune subsets, they do not systematically cover subsets across immune cell types, or over longer delays.

The stability of most major subsets after a delay of 24 h to PBMC processing indicates that immune profiling of

Received 20 October 2023; Revised 20 February 2024; Accepted for publication 26 April 2024

certain populations, or subsets thereof, may be accurate with longer delays. In this study, we sought to understand the impact of such delays by applying an extensive 44-parameter cytometry by time-of-flight (CyTOF) immunophenotyping panel to blood samples processed same-day and after up to 7 days delay, including alternative anticoagulant and storage conditions. The study incorporated both healthy adults (HA) across a range of ages and rheumatoid arthritis (RA) subjects to include diversity of immune health. This information can be used to determine which subsets and markers are stable or sensitive to certain processing delay lengths.

Materials and methods

Blood collection and conditions

Venipuncture was performed on five HA and two RA subjects (Fig. 1A). Samples were collected from subjects under approval at the Benaroya Research Institute under IRBs 10059

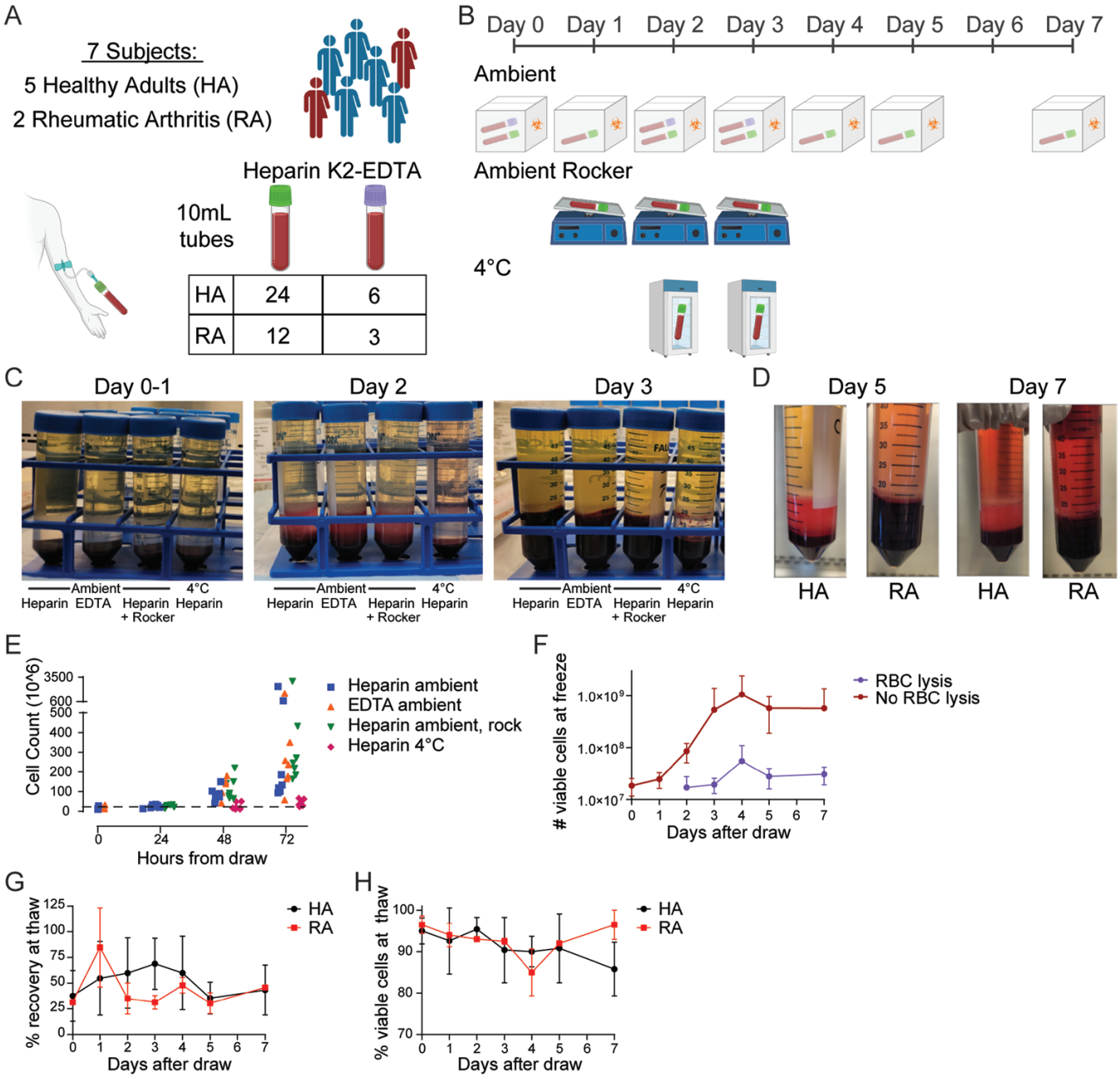

Figure 1. Delays to PBMC processing impact Ficoll separation and recovery of viable cells. (A) Whole blood was collected from five HA and two RA patients into a mix of Hep and K-EDTA tubes. (B) Blood was stored in collection tubes for an indicated number of days in ambient shipping containers, ambient on a rocker, or in a 4°C refrigerator. PBMC were isolated using a Ficoll gradient after the storage period. (C) Representative photos of HA Ficoll gradients with processing at Days 0–3. Storage condition is indicated below the images. (D) Representative photos of HA and RA Ficoll gradients at Days 5 and 7. (E and F) Cells were counted after the completion of Ficoll gradients. (E) Counts without RBC lysis in each storage condition out to Day 3. (F) Total number of viable cells prior to cryopreservation from the heparin ambient condition with or without RBC lysis. (G and H) Upon thaw, cells were treated with DNase and RBC lysis prior to counting. (G) % of cryopreserved cells recovered upon thaw relative to counts with RBC lysis at cryopreservation. (H) % viable of cells after thaw. (F–H) Points depict the mean and error bars depict the standard deviation

(RA subjects) and 3 041 700 (healthy adults). Whole blood was collected from the HA into 30 × 10 ml tubes (BD)—24 containing heparin (Hep) with either Li or Na and 6 with dipotassium ethylenediaminetetraacetic acid (K2 EDTA), for a total of 300 ml.

One hundred fifty milliliters were collected from the RA subjects into the same ratio of 10 ml Hep and K2 EDTA tubes. Samples were divided into three different storage conditions: ambient in an ambient shipping container, ambient on a rocker, and 4°C, and then processed for PBMC over a 7-day span (Fig. 1A).

PBMC processing

Whole blood was processed into PBMC according to the schedule outlined in Fig. 1B. Ten mL of blood was added to a 50 ml conical polypropylene tube (Corning, Cat. 430291) and diluted with 30 ml of phosphate-buffered saline (PBS, Sigma–Aldrich, Cat. D8537). After gently mixing, 12 ml of Ficoll-Paque Plus (Cytiva, Cat. 17144003) was underlaid and tubes were centrifuged at 1000× *g* for 30 min with no brake. The resulting PBMC layer was collected into a new 50 ml tube and washed with washing solution (1% Human AB (HuAB) serum in PBS, GeminiBio, Cat. 100–512). Samples were centrifuged at 400× *g* for 10 min with low brake, the supernatant was aspirated, and cells were resuspended in 20 ml of washing solution for enumeration. An additional 30 ml of washing solution was added to samples and centrifuged a final time at 400× *g* for 10 min with a high brake.

Cell counting

Cells were counted on Countess III (Invitrogen, Cat. AMQAF2000) after mixing sample 1:1 with Trypan Blue (Invitrogen, Cat. T10282). On and after Day 2, a 50 µl aliquot of each ambient sample was collected and treated with 450 µl of VersaLyse (Beckman-Coulter, Cat. A09777) prior to preparing for counting.

PBMC cryopreservation

PBMC pellets were resuspended in HuAB serum for half volume and 20% dimethylsulfoxide (DMSO, Corning, Cat. 25-950-CQC) in HuAB serum for a final 10% DMSO freezing solution. Volumes were determined to allow up to three cryovials for RA subjects and five for HA, with approximately 5×10^6 cells per tube. One milliliter of each sample was aliquoted into each cryovial (ThermoFisher, Cat. 368632) and placed in a Mr. Frosty (ThermoFisher, Cat. 5100-0001) in a −80°C freezer for 16–72 h. Afterward, samples were transferred to liquid nitrogen storage.

Sample thawing

After 2 months in storage, one sample from each of the 15 conditions for a single subject was pulled from liquid nitrogen and placed on dry ice. Vials were thawed in a 37°C water bath until only a pea-sized amount remained frozen, then transferred to 50 mL conical tubes. One milliliter of a pre-warmed 10% HuAB serum (Access, Cat. 515-HI) in RPMI-1640 (Cytiva, Cat. SH30255.01) supplemented with sodium pyruvate, L-glutamine, and penicillin–streptomycin (thawing media) was added dropwise to each sample, followed by rinsing the cryovial with an additional 1 ml and adding dropwise to gently dilute the DMSO. Rocking the 50 ml conical gently, another 7 ml of thawing media was added dropwise, and topped off to a total volume of 20 ml. The samples were then centrifuged at 400× *g* for 5 min, and the supernatant was aspirated from the resulting pellet. Each sample was treated with 2 ml of 1× red blood cell (RBC) Lysis Buffer (Biolegend, Cat. 420301) for 5–15 min, depending on the level of red blood cell contamination, and centrifuged again for 3–5 min. The supernatant was aspirated from each cell pellet and cells were resuspended in 2 ml of a 1:5000 benzonase nuclease (Sigma–Aldrich, Cat. E1014) in thaw media solution prior to performing a post-thaw cell count. Once counted, 3 ml of additional thaw media was added to each sample and centrifuged a final time at 400× *g*. Samples were resuspended at a concentration of 10×10^6 cells/ml in thaw media and 10^6 cells plated in a 96-well round-bottom plate (ThermoFisher, Cat. 163320) for CyTOF staining.

Barcoding strategy

Samples from the same subject were barcoded and combined for CyTOF staining and acquisition to reduce technical variability. Samples from each subject were divided into two barcode pools, as follows: Barcode pool 1 consisted of all samples from the Hep RT storage condition (Days 0–5, 7), and an internal PBMC batch control. Barcode pool 2 consisted of all other conditions and days from the subject (Hep RT rock days 1–3; Hep 4°C days 2–3; and EDTA RT days 0, 2–3) as well as a replicate Hep RT Day 0 sample. A combinatorial barcoding approach was used, in which each sample was dual-stained with a unique combination of CD45 metal-labeled antibodies and then combined for all downstream CyTOF staining and acquisition (Supplementary Table S1).

CyTOF Staining

Samples were divided into four batches for CyTOF staining and acquisition. Batches consisted of one to two subjects and all of their conditions and timepoints. All batches were stained and acquired over a period of approximately 1 week, with no more than one batch stained per day. Surface and intracellular antibody staining cocktails (Supplementary Table S2) were prepared in bulk and divided into single-use aliquots frozen at −80°C prior to the beginning of the study to reduce technical variability. Cells were incubated with metal-labeled CD45 antibodies according to the barcoding strategy described above for 20 min and then washed and combined into one well per barcode pool for remaining staining and acquisition steps. Cells were then stained for viability using 100 µl of 1 µM niobium chloride solution (Sigma–Aldrich) for 5 min and quenched with cell staining buffer (Standard BioTools). Cells were washed and then stained with 200 µl surface antibody staining cocktail and incubated in ambient conditions for 20 min, followed by a wash and spin for 3–5 min at 300× *g*. Cells were then fixed using the Maxpar Nuclear Antigen Staining Buffer (Standard BioTools) for 20 min in ambient conditions, and stained with 200 µl intracellular antibody staining cocktail for 30 min in ambient conditions. Following a wash and spin for 3–5 min at 400× *g*, cells underwent a 10 min incubation with 1 ml of 1.6% PFA in PBS (Santa Cruz Biotechnology). Cells were then washed and spun for 3–5 min at 400× *g* and resuspended in 1 ml 0.125 µM Iridium Intercalator solution (Standard BioTools) and stored at 4°C until acquisition. Samples were acquired on the CyTOF within 3 days of staining.

CyTOF acquisition

On the day of acquisition, cells were washed with 0.5 ml Cell Staining Buffer (Standard BioTools), followed by 0.5 ml ultrapure water, and then kept in pelleted form on ice. Immediately prior to acquisition, cells were resuspended in a solution of EQ Four Element Calibration Beads (Standard BioTools) diluted 5-fold into ultrapure water and passed through a 35 µM cell strainer (Falcon) before being introduced to the instrument. Samples were acquired on a CyTOF Helios (Standard BioTools) and collected in their entirety at an event rate no greater than 600 events per second. FCS files were randomized and normalized for EQ Bead intensity using the CyTOF Software v 7.0.8493.

De-barcoding and manual gating

Following the acquisition, barcoded FCS files were loaded into FlowJo v 10.5.3 (BD, Ashland, OR). Samples were first gated on cells (DNA+, beads–), singlets (DNA+, consistent event length), and then live (DNA+, niobium chloride–). Single gates for each of the five CD45 metal-labeled antibodies used were created for each sample. Boolean combination gates were then created to reflect the combinatorial barcodes and recapitulate the original samples. De-barcoded samples were given a unique identifier and exported, such that the storage condition (tube type, temperature, and day) and subject type (HA or RA) for each subject were blinded for unbiased analysis. Exported FCS files were re-loaded into FlowJo v 10.8, and then gated by blinded personnel as indicated in Fig. 2. Gates were checked for consistency within the individual and confirmed by other personnel, and frequencies were exported to Excel (Microsoft, Redmond, WA). At this time, output frequencies were unblinded for comparison between conditions. FCS files were exported for the CD66b–CD3–CD19–, CD66b–CD3+ CD19– T cell, and CD66b–CD3–CD19+ B cell populations for clustering analysis.

Statistics and computational analysis

Unblinding was completed by matching Excel output frequencies from the blinded gates to an unblinding key.

Calculations including mean, standard deviation, and *Z*-score were computed in Excel. Graphs were generated and statistics including simple linear regression and Friedman test with Dunn's multiple comparisons test computed in GraphPad Prism 10.0.0 (GraphPad).

The Distribution analysis across clusters of a parent population overlaid with a rare subpopulation (DISCOV-R) R package ([24], and https://github.com/BenaroyaResearch/briDiscovr) was used for clustering analysis and marker intensities on non-granulocyte gated live cells, and to generate heatmaps and uniform manifold approximation and projection (UMAP) plots.

Results

Red blood cell contamination reduces the separation of leukocytes by 2 days delay in processing

To determine the impacts of delays in PBMC processing on immunophenotyping, we collected blood from five HA and two RA subjects in two types of tubes (Fig. 1A, Table 1) under three specified storage conditions (Fig. 1B) for up to 7 days. Following isolation of PBMC using Ficoll gradients we observed visible RBC contamination of the buffy coat layer by Day 2 in all conditions, though storage at 4°C decreased the RBC contamination on Day 2 (Figure 1C). Contamination increased to Day 3 (Figure 1C) but was decreased by doubling the dilution factor of the blood in the gradient. While contamination was consistent between HA and RA subjects out to Day 4 (data not shown), by Day 5, RBC contamination was noticeably greater in RA subjects than HA (Fig. 1D).

To measure the impact at the cellular level, we counted cells both prior to (Fig. 1E and F) and after (Fig. 1G and H) cryopreservation. Prior to cryopreservation, counts became more variable out to Day 3 (Fig. 1E). Consistent with the visual improvement in RBC contamination, storage at 4°C also improved the consistency of cell counts of delayed samples. In contrast, other conditions showed similar variability of counts (Fig. 1E). Total pre-freeze counts were increased >10-fold, an increase explained by RBC contamination (Fig. 1F). In contrast, total counts were largely stable after RBC lysis. Percent viable prior to cryopreservation became more variable by Day 3 (data not shown). Percent recovery after thaw was generally maintained across the time series (Fig. 1G). Viability of thawed cells was above 80% in the majority of subjects even with delays of up to 7 days, though there was a trend toward decrease over time (Fig. 1H).

Delays of four or more days to processing decreased monocytes

As the apparent stability of cell numbers and viability may obscure subtler changes in subpopulations, we performed extensive immune profiling. We barcoded and pooled samples (Supplementary Table S1) and analyzed them by CyTOF (Supplementary Table S2) to identify various immune populations and subsets of interest in clinical immunology studies. Manual gating identified major immune populations including T cells, B cells, NK cells, and myeloid cells (Fig. 2A). These populations were all gated as percentage of CD66b– cells because the decreased quality of Ficoll isolation increased the contamination by CD66b+ neutrophils and other granulocytes (Fig. 2B). Major immune populations were analyzed over the time course in each individual (Fig. 2C and D). The most notable change was a decrease in the frequency of monocytes (Fig. 2C), while dendritic cells (DC), B, T, and NK cells were relatively stable (Fig. 2D). Stability varied between subjects (Fig. 2C and D), but with similar trends overall. The decrease in monocytes became apparent in all subjects by Day 4, but changes to a smaller degree and in fewer subjects are clearly observable by Day 2 (Fig. 2C and D). When storage conditions were compared, the drop in monocytes was most marked in EDTA tubes, while the ambient heparin condition had the greatest stability across major populations (Fig. 2E).

Variation in immune populations increases with a delay in processing

To normalize changes across subjects and establish at which days major subset frequencies became substantially variable, we calculated mean and standard deviation of each population frequency within subject at Days 0–1 in the heparinized samples. We focused on ambient heparinized samples for analysis in time points beyond Day 3 because they demonstrated the greatest stability in the initial analysis from Days 0–3 (Fig. 2E). For Days 2–7, we then calculated the difference from the baseline mean (Fig. 3A). The heatmap depicts whether values

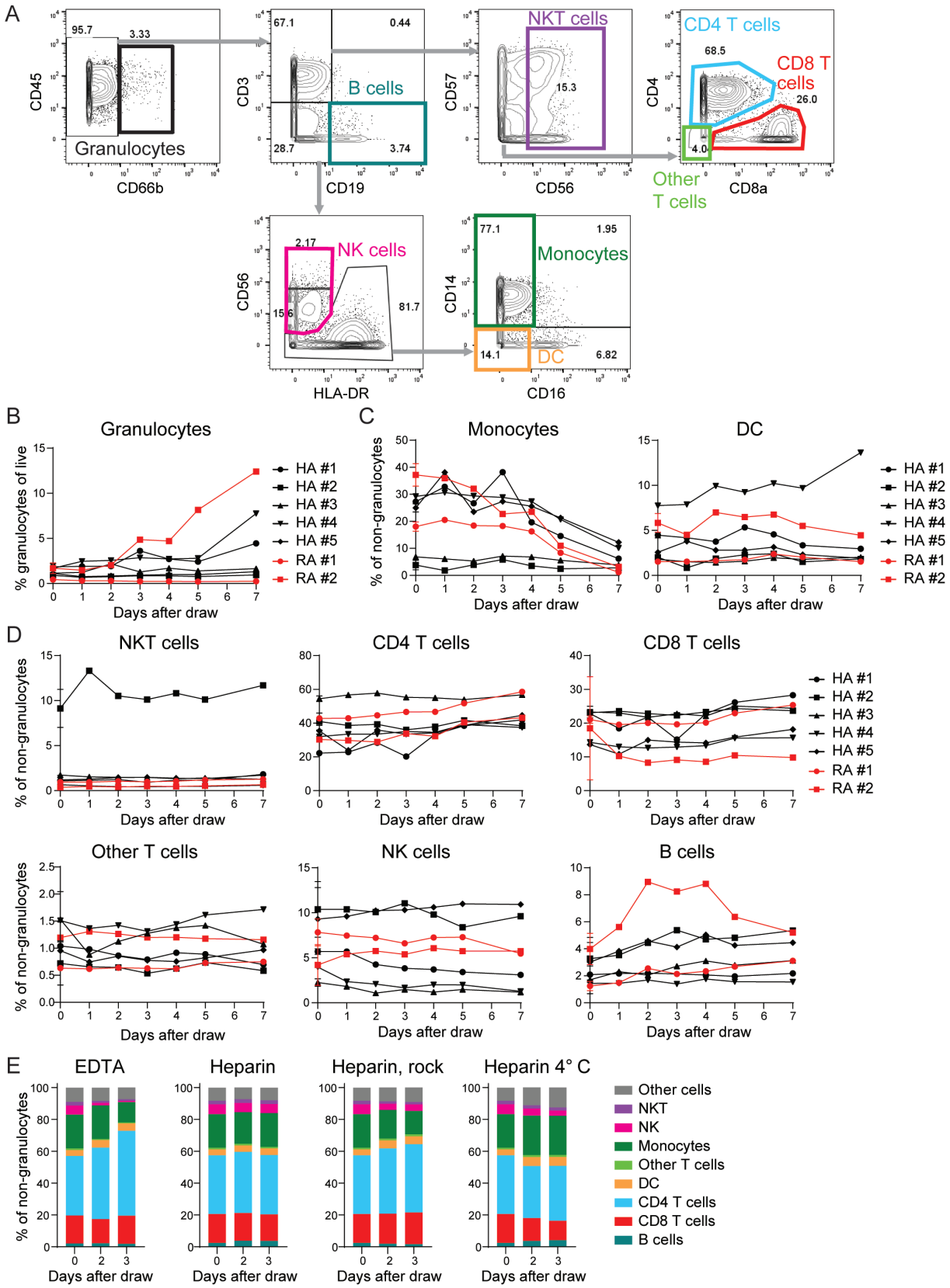

Figure 2. Monocytes are most impacted by delays in processing. (A) Thawed samples were analyzed by mass cytometry and gated for live singlets as indicated. (B) Granulocytes, (C) myeloid cells, and (D) other leukocyte subsets were analyzed over time in HA and RA subjects in Heparin room temperature samples. Each individual subject is represented with a distinct symbol, as indicated in the figure. (E) Non-granulocyte gated cells (CD66b−) were analyzed for each condition at Days 0, 2, and 3 for frequencies represented by each population. Other cells = all cells that do not fall into the gated populations. This includes some subsets of non-classical monocytes and DCs, double-positive T cells, innate lymphoid cells, and cell–cell conjugates

Table 1. Subject demographics

Subject ID	Patient type	Age at Draw	Sex	Race	Ethnicity	Treatment
HA #1	Healthy	38	F	Asian	Not Hispanic/Latino	N/A
HA #2	Healthy	50	F	Asian	Not Hispanic/Latino	N/A
HA #3	Healthy	26	F	White	Not Hispanic/Latino	N/A
HA #4	Healthy	36	F	White	Not Hispanic/Latino	N/A
HA #5	Healthy	50	M	White	Not Hispanic/Latino	N/A
Internal Control	Healthy	69	F	White	Not Hispanic/Latino	N/A
RA #1	RA	52	F	White	Not Hispanic/Latino	Ibuprofen, Prednisone
RA #2	RA	66	M	White	Not Hispanic/Latino	Ibuprofen

at indicated time points were within 2 SDs of the mean at baseline. All subsets varied by >2 SDs in at least one subject by Day 2, with variation affecting increasing numbers of subjects and number of subsets within subject over time (Fig. 3A). All subsets were affected in two or more subjects at Day 7 (Fig. 3A). B cells were impacted by Day 2, with extensive variation visible by Day 3, particularly in the two subjects with RA (Fig. 3A). We also quantified variation of each subset by calculating the total of subject/time points with >2 SDs for each subset, as shown in the far right column, demonstrating impacts on all subsets. In addition, we quantified variation of each subject/time point in the same manner (bottom row), which demonstrated variation present at Days 2–4, with increased variation in six of seven subjects on Days 5 and 7 (Fig. 3A).

To incorporate directionality of change, we calculated *Z*-scores relative to baseline mean for each population in each subject at each time point (Fig. 3B). From Days 1 to 3, variation was not affected by heparin versus EDTA coagulant or by storage condition (two-way ANOVA, $P = 0.32$). The decrease in monocytes was apparent in all subjects by Day 4, as was an increase in CD4 T cells (Fig. 3B). Several subsets had evidence of increased variability as early as Day 2, including DC and other T cells, though their directionality was not consistent across subjects (Fig. 3B). To understand how variation in subsets differed from subject to subject, we also visualized *Z*-scores for individual subjects (Fig. 3C). Two of the 5 HA (HA #1 and HA #4) and both RA subjects had substantial variation in some subsets. Across these four subjects, the greater variation was apparent by Day 2 and increased in later days. In contrast, three of the HA subjects had largely stable *Z*-scores (Fig. 3C). Thus, variability can increase by as early as 2 days, but some samples may be more robust.

Both classical and non-classical monocytes are depleted by delays in processing

Given the change in monocytes with delay in processing, we investigated whether there were any impacts on smaller innate leukocyte subsets. To minimize variation induced by gating, we performed clustering on CD66b–CD3–CD19– cells (Supplementary Fig. 1A and B). The clustering identified subsets of monocytes, DC, and NK cells, as well as basophils (Fig. 4A). Both classical and non-classical monocytes decreased (Fig. 4B, $P < 0.01$), with changes from Days 0–7 for classical monocytes ($P = 0.027$), and from Day 0 to Days 4–7 for non-classical monocytes ($P < 0.001$). Basophils had a non-statistical trend toward decrease (Fig. 4C, $P = 0.06$). Conventional (c)DC1 also decreased ($P < .05$), while cDC2 had no change and plasmacytoid (p)DC had a non-statistical trend toward decrease ($P = 0.1$, Fig. 4D). However, pDC had a decrease from Day 0 to 5 and 7 ($P < 0.05$). CD56bright and proliferating NK cells were stable, while there was a non-statistical trend towards an increase in CD56dim NK cells (Fig. 4E, $P = 0.06$). The observed trends were consistent across subjects (Fig. 4B–E).

Plasmablasts decreased while memory B-cell subsets increased with delays in processing

The analysis of CD66b–CD3–CD19– cells demonstrated that there were changes in innate subsets with delays to processing that were obscured in the analysis of global subsets. Accordingly, we completed a similar analysis on CD66b–CD3–CD19+ B cells (Supplementary Figure 1C, and D), which identified six clusters of naïve and memory B cells, as well as plasmablasts (Fig. 5A). Naïve B cells were maintained, while plasmablasts decreased (Fig. 5B, $P = 0.005$), specifically from Days 0 to 3–7 ($P < 0.05$). In contrast, CD27– memory B cells increased (Fig. 5B, $P = .03$), with statistical changes from Days 0 to 2–7 ($P < .05$). Trends were consistent across all subjects (Fig. 5B). While total B cells are preserved with delays to processing, particular B-cell subsets are impacted much earlier.

Follicular helper T cell and Th17 subsets were differentially impacted by delays in processing

To further analyze changes in immune subsets, we clustered CD66b–CD3 + CD19– T cells (Supplementary Figure S1E and S1F) and identified CD4, CD8, mucosal-associated invariant T (MAIT), γδ, double negative (DN), and NK T cells including regulatory T cells (Treg) and memory and naïve subsets (Fig. 6A). The majority of innate-like subsets were stable, but a subset with a Helios + NK-like phenotype had a non-statistical increase (Fig. 6B and C, $P = .06$). CD8 and CD4 subsets were likewise predominantly stable (Fig. 6D and E). Naïve CD4 T cells had an increase from Day 0 to 5–7 ($P < 0.01$), and Treg had a decrease from Day 0 to 3–7 ($P < 0.05$). The majority of trends were consistent between subjects, with elevated subject-to-subject variation for CD4 cytotoxic and CD4 "exhausted" subpopulations. The CD4 memory cluster had a non-statistical increase (Fig. 6F, $P = 0.06$) and comprised a heterogeneous population, so we extracted and reclustered that population to identify T helper (Th) subsets (Fig. 6G). Follicular helper T cells (Tfh) decreased with delays to processing, specifically from Day 0 to 4–5 ($P < 0.05$), while Th17 had a trend toward reciprocal

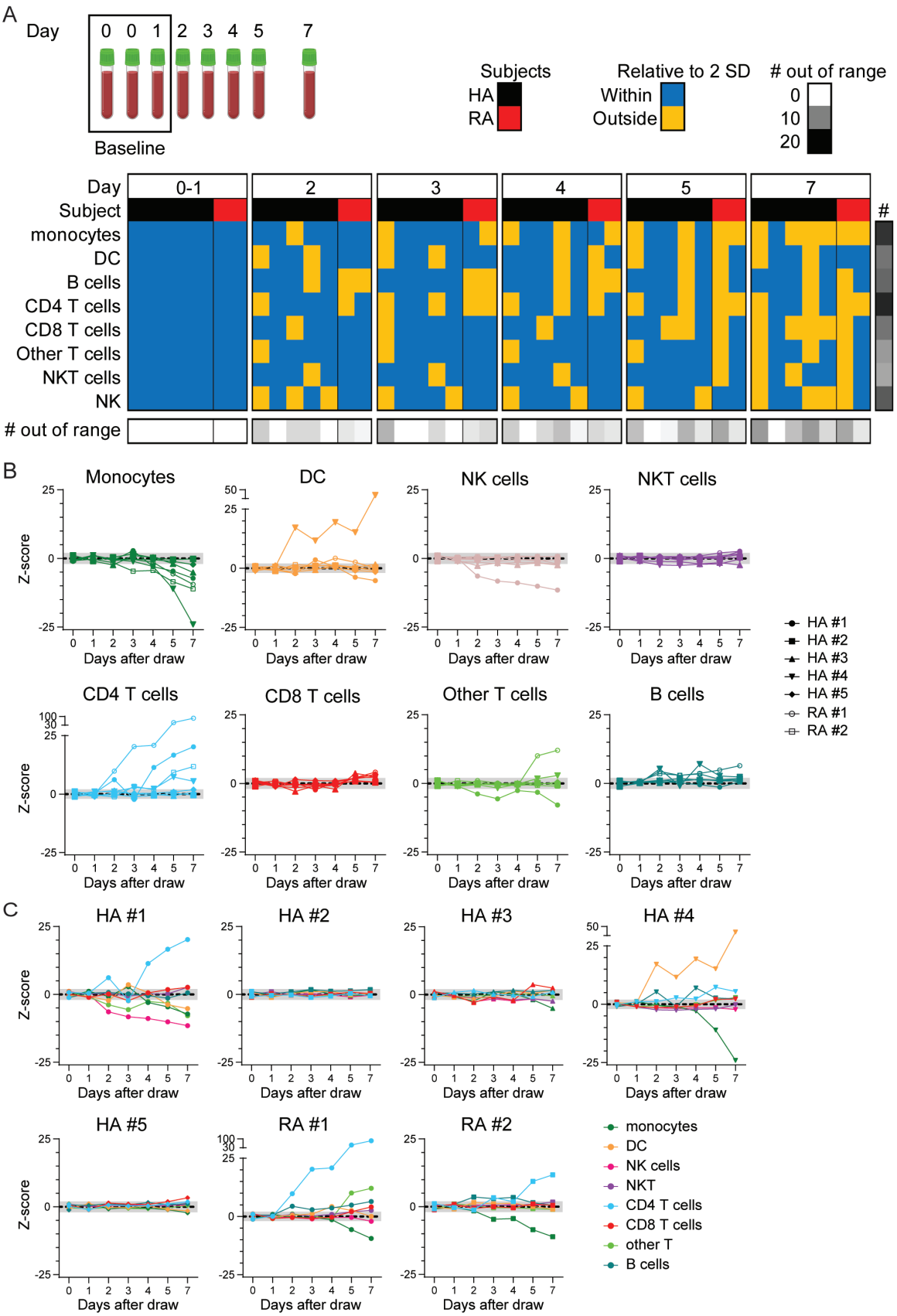

Figure 3. Variability of immune population frequencies increases by Day 2. For heparin samples stored in ambient conditions, baseline mean, and standard deviation for each population frequency from Fig. 2A for each subject were calculated using Days 0–1. (A) Heatmap depicts populations with frequencies within and outside two standard deviations from the mean as indicated in the key for the figure. Grayscale bars depict number of populations out of range within subject/day (bottom) and within population (right). (B and C) Number of standard deviations from the mean at baseline (*Z*-score) calculated for each HA and RA subject and population at each time point depicted for (B) each population and (C) each subject. Points are connected by lines within (B) subject or (C) population. Dotted line indicates 0, and shaded box indicates the range of 2 SDs from 0. Each subject is indicated with a distinct symbol

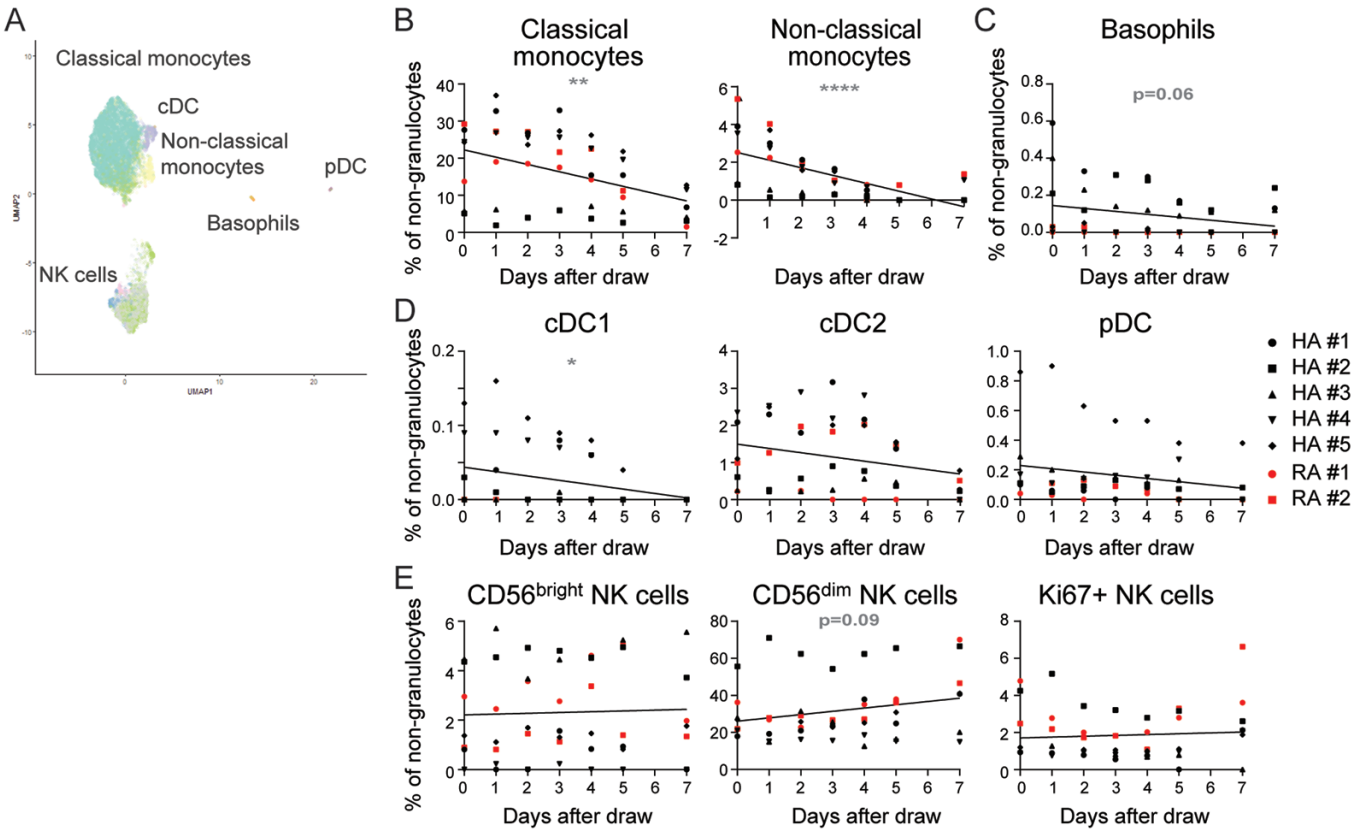

Figure 4. Both classical and non-classical monocytes are decreased with delays in processing. (A) CD66b−CD3−CD19− cells gated as shown in Fig. 2A were clustered using DISCOV-R based on the listed parameters (Supplementary Figure S1A and SB), with the clusters projected onto a UMAP. Population names were determined based on protein expression patterns. The frequency of each cluster over the time course in Heparin ambient storage samples from barcode set 1 was analyzed for (B) monocytes, (C) basophils, (D) dendritic cell subsets, and (E) NK cell subsets. Each HA and RA subject is indicated with a distinct symbol. Statistics displayed on graphs computed using simple linear regression. Statistics computed between time points (in text) with Friedman test with Dunn's multiple comparisons test. * = $P < 0.05$, ** = $P < 0.01$,**** = $P < 0.0001$

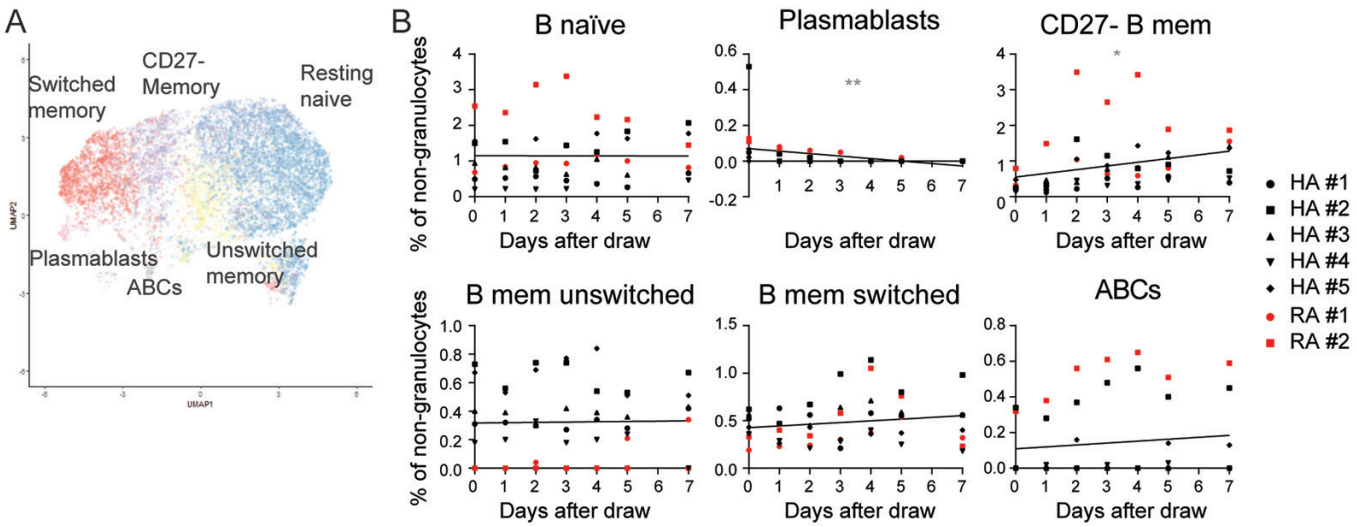

Figure 5. Plasmablast and memory B cell subsets shift with delays to processing. (A) CD66b-CD3-CD19 + B cells gated as shown in Fig. 2A were clustered using DISCOV-R based on the listed parameters (Supplementary Figure S1C and D), and clusters were projected onto a UMAP. Population names were determined based on protein expression patterns. The frequency of each cluster over the time course in Heparin ambient storage samples from barcode set 1 was analyzed for (B) naïve B cells, memory B cells, plasmablasts, and age-associated B cells (ABCs). Each HA and RA subject is indicated with a distinct symbol. Statistics displayed on graphs computed using simple linear regression. Statistics computed between time points (in text) with Friedman test with Dunn's multiple comparisons test. * = $P < 0.05$, ** = $P < 0.01$

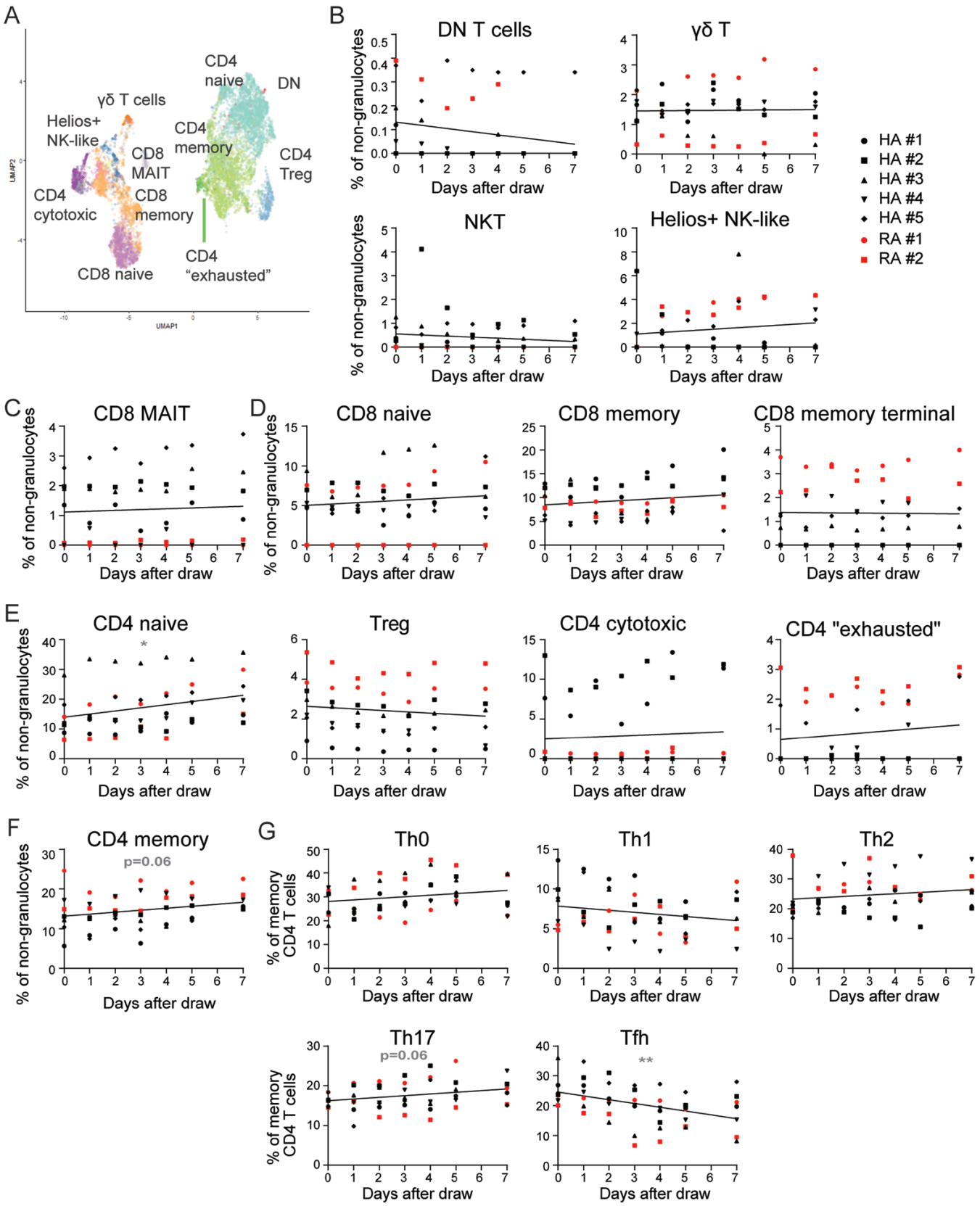

Figure 6. Tfh cells were depleted by delays to processing, while Th17 cells were preferentially preserved. (A) CD66b−CD3+ CD19− T cells gated as shown in Fig. 2A were clustered using DISCOV-R (Supplementary Figure S1E and S1F) and clusters were projected onto a UMAP. Population names were determined based on protein expression patterns. The frequency of each cluster over the time course in Heparin room temperature samples from barcode set 1 was analyzed for (B) innate-like T-cell subsets, (C) MAIT cells, (D) CD8 T-cell subsets, (E) CD4 T-cell subsets, and (F) CD4 memory T cells. (G) CD4 memory cluster from Fig. 6A was exported and DISCOV-R clustering was run on this subset based on the Th lineage-defining markers CCR4, CCR5, CXCR3, and CXCR5. Population names were determined based on protein expression patterns. Frequency of each Th cluster over the time course analyzed. Each HA and RA subject is indicated with a distinct symbol. Statistics displayed on graphs computed using simple linear regression. Statistics computed between time points (in text) with Friedman test with Dunn's multiple comparisons test. ** = $P < 0.01$

increase (Fig. 6G, $P = 0.06$). Th0, Th1, and Th2 subsets were stable. The trends in these subsets appeared to be consistent between subjects.

Activation, homing, co-stimulation, and proliferation markers altered by delays in processing

The analysis thus far demonstrates extensive impacts of delayed PBMC processing on immune subsets but does not identify changes in non-lineage-defining markers, many of which are associated with cellular function. Several of these markers, particularly chemokine receptors, are already known to have altered expression in the context of processing delays [9, 13]. We measured relative expression of chemokine receptors and markers associated with lymphocyte activation on naïve-excluded CD4 and CD8 T cells, Treg, B cells, monocytes, cDC, and NK cells (Fig. 7). In comparison to Day 0, expression of activation markers (Fig. 7A), chemokine receptors, and other markers (Fig. 7B) was altered as early as Day 2, with changes increasing with further delays. The majority of proteins had distinct changes in Treg relative to all other populations, including the CD4 and CD8 T-cell populations. Several proteins increased in monocytes concurrent with the depletion of the population. The changes in protein expression were also not consistent across subsets. For example, HLA-DR, CD95, CD38, ICOS, CCR7, CXCR3, and Ki67 changed across the majority of subsets ($P < 0.05$), and CD25 and CD27 were stable in most subsets but decreased in B cells ($P < 0.0001$) and monocytes ($P < 0.01$), while PD1 and CD56 changed only in monocytes ($P < 0.0001$). While detected by Day 2 ($P < 0.05$), the changes in marker expression increased in magnitude in most subjects by Day 3. Overall, even among immune subsets preserved after delays to processing, increased variability of expression limits the interpretability of data from specimens with delayed processing as early as Day 2 (Fig. 8). The distinct impacts of delayed processing on each immune population at each time point led us to generate a flow chart to aid in decision making depending on the magnitude of delay and experimental requirements (Fig. 8).

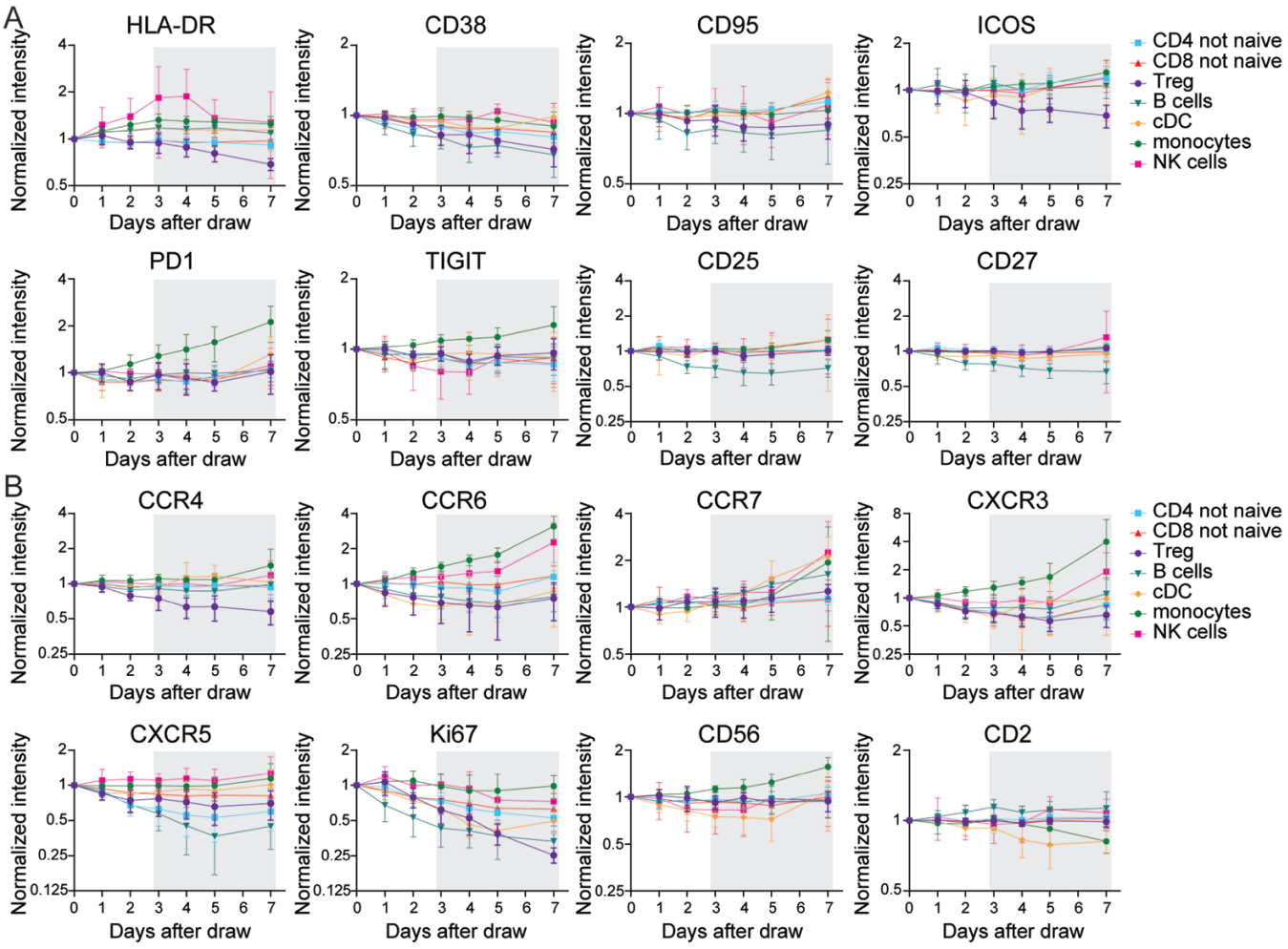

Figure 7. Expression of activation and other markers was altered by two or more days of delay to processing. DISCOV-R clusters for non-naïve (not CCR7+ CD45RA+) CD4 and CD8 T cells, Treg, B cells, cDC, monocytes, and NK cells were analyzed for the median intensity of expression of (A) proteins known to change with activation and (B) other proteins including chemokine receptors in Heparin ambient storage samples from barcode set 1. Intensities were normalized to the intensity at Day 0 and plotted in log2 scale. Proteins analyzed were (A) HLA-DR, CD38, CD95, ICOS, PD1, TIGIT, CD25, and CD27, (B) CCR4, CCR6, CCR7, CXCR3, CXCR5, Ki67, CD56, and CD2. Shaded boxes highlight Days 3–7 after the draw. Statistics were computed using simple linear regression (for each subset). Statistics computed between time points with Friedman test with Dunn's multiple comparisons test. All statistics are shown in the text only

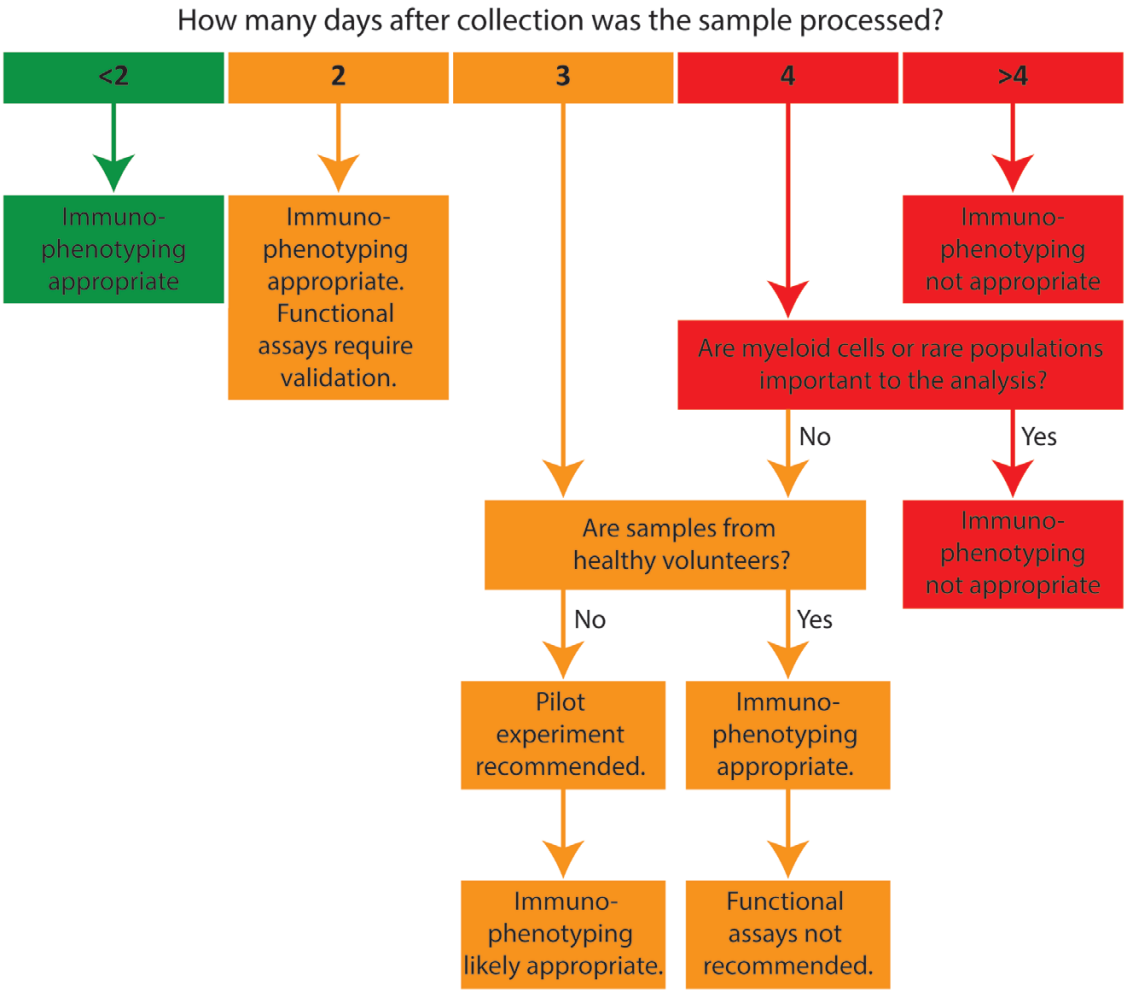

Figure 8. Decision tree for use of samples with delayed processing. Based on the results of this study, this decision tree provides guidelines on how to determine whether samples with 2–7 days delay in processing are appropriate for use in specific experiments. Color coding of boxes and arrows demonstrates recommendations for use. Samples processed within 2 days are appropriate for use in an immune profiling study. For samples processed 2-3 days after collection, further validation is recommended. Samples processed 4 or more days after collection are not recommended for use

Discussion

Immunophenotyping of peripheral blood lymphocytes is an important tool for mechanistic analysis in immunotherapy clinical trials as well as in studies of disease development and biomarkers in human subjects. Study logistics often require that blood be shipped from the clinical site to a laboratory for processing, which can lead to significant delays in processing. We sought to understand the impact of such delays through CyTOF immunophenotyping in adults across a wide age range and both health and disease, with up to 7 days delay to processing. The primary impact on major immune subsets out to 7 days was a decrease in monocytes. Expression of activation markers and chemokine receptors also changed by Day 2, indicating earlier impacts on cellular function and quality than survival.

While prior studies have addressed the effect of delays to PBMC processing on cell quality, this study is novel in several key ways. First, the majority of studies have analyzed immune cell composition after delays of 24 h or less [4, 16, 17, 20, 21]. The exceptions focused on a variety of immune subsets, with mixed results [4, 5, 10]. To the best of our knowledge, ours is the first study to analyze immunophenotyping of blood cells after delays beyond 3 days. Second, the majority of published analyses of PBMC delays focused exclusively on healthy adults. The inclusion of RA subjects in our study gives a more representative picture of the impacts of PBMC processing delays in diverse patient populations. Third, the use of CyTOF enabled both broad analysis across immune cell types and identification of impacts on many specific subsets. In combination, these features allowed us to determine that there were changes not only in classical monocytes but also in non-classical monocytes, Tfh, and plasmablasts. Fourth, the experimental design allowed direct comparison between different anticoagulants and storage conditions, which identified that none of the analyzed storage conditions mitigated the impacts of delayed processing. In combination, these features of our study allowed us to determine that while the yield and viability of PBMC varied, the frequencies of many subsets were stable for up to 4 days.

In this study, the most robust effect of delayed processing was the decrease of monocytes. Published findings suggest intriguing hypotheses for the cause. Delays of as little as 2 h to PBMC processing can increase the levels of monocyte-platelet aggregates and shift the proportions of monocyte

subsets [23]. Additionally, if delays cause monocytes to become more likely to stick to the walls of the Ficoll tube or cryovial, either because they aggregated with platelets or for some other reason, that would also result in a decreased frequency of monocytes. Classical monocytes are also known to have a short half-life in circulation (~1.6 days), while non-classical monocytes have a slightly longer half-life (~7 days) [25], in contrast to T cells, which commonly live for months [26]. Thus the relative decrease in monocytes could reflect the fact that monocytes simply have shorter lifespans than B or T cells.

In addition to the decrease in both monocyte subsets, subsets of B and T cells were impacted, including plasmablasts and Tfh cells. Due to the small frequencies of these populations, stochasticity could be a major factor in changes in the populations. Differential survival could be another factor. Tfh may be more susceptible to apoptosis than naïve or memory T cells [27]. Plasmablasts similarly represent a short-lived population. Additionally, delays to processing could impact the expression of markers; chemokine receptors such as CXCR5 are particularly sensitive to many changes in samples [13].

Even among stable CD4 and CD8 effector T-cell populations, changes in activation markers were observed with delays to processing. For each activation marker, the directionality of changes varied, and the changes in CD4 non-naive, CD8 non-naive, and Treg were distinct. Activation markers expressed in different patterns may lead to differential predispositions to cell death. Alternatively, the expression of activation markers may have been altered by delays to processing—granulocytes are known to activate with delayed processing, and to thereby affect T-cell activation [20]. Additionally, the loss of monocytes alters antigen presentation to T cells, which may also affect their activation state. There are many possible causes for the change in activation states, but ultimately these data demonstrate that 2 days after collection activation states no longer represent the *ex vivo* status at Day 0. It is likely impossible to interpret activation states from T cells processed three or more days after collection.

A few factors are important to contextualize our findings of the impact of delays to processing on immunophenotyping. First, our study cohort represents a mixture of healthy adults across a range of ages and RA subjects. While this gave a representative picture of how delayed processing can affect samples over a spectrum of immune states [28, 29], we were not powered to make statistical comparisons by disease state or age. Second, the use of CyTOF provides in-depth data on protein expression, but RNA expression may be affected quite differently. A recent study demonstrated that delays of less than 24 h to processing have impacts on transcriptional expression not reflected in immune profiling [19]. We therefore recommend further studies to address the impact on RNA. Third, we did not exhaustively investigate the impacts of different anti-coagulants and storage conditions. Our study did not address the potential impacts of higher temperatures or temperature changes that can occur with the shipment of ambient pack samples [8, 13, 20]. Fourth, we did not measure the impacts of delayed processing on fresh PBMC. Our use of cryopreserved PBMC with batched CyTOF analysis limited technical variability as a factor in our study. However, the use of fresh versus frozen PBMC is known to impact some immunophenotypes [30], so analysis of those immunophenotypes in fresh samples will need to be completed separately. In addition, studies of fresh PBMC across multiple batches will likely have higher technical variation than that experienced in our study. Fifth, even after minimizing variability in processing, including keeping the operators and reagent lots consistent over the entirety of the study, we observed substantial variation in cell counts prior to cryopreservation, even after RBC lysis. We suspect this is due to inconsistent granulocyte contamination, which is known to increase with delayed processing, but then is largely lost after cryopreservation. Further testing may address the extent to which processing delays increase technical variation.

In conclusion, this study provides an in-depth analysis of the impacts of delayed PBMC processing on immunophenotyping, both for the frequency of subsets as well as quality. The most depleted population was monocytes, with small lymphocyte subsets, including plasmablasts and Tfh, and expression of activation markers and chemokine receptors impacted as well. Based on these findings, extreme caution is recommended in interpreting data from samples with greater than 4 days delay to processing. Samples with 2–4 days delay to processing can still be informative, with the caveat that some subsets are sensitive even at early timepoints. These data confirm the widely accepted recommendation that PBMC should be processed as soon as possible after blood collection but also provide options for using delayed samples when necessitated by study design or limitations.

Supplementary Data

Supplementary data is available at *Clinical and Experimental Immunology* online.

Acknowledgements

We would like to thank the Benaroya Research Institute Center for Interventional Immunology for subject enrollment and sample collection, and the Biomarker and Discovery Research group at the Immune Tolerance Network for feedback on study design and the manuscript.

Ethical Approval

Samples were collected from subjects under approval at the Benaroya Research Institute under IRBs 10059 (RA subjects) and 3041700 (healthy adults).

Conflict of Interests

The authors have no conflicts of interest to disclose.

Funding

Research reported in this publication was supported by the National Institute of Allergy And Infectious Diseases of the National Institutes of Health under Award Number UM1AI109565. The content is solely the responsibility of the authors and does not necessarily represent the official views of the National Institutes of Health.

Data Availability

Data are available on ITN TrialShare (https://www.itntrialshare.org/) under protocol #ITN917AI (https://www.itntrialshare.org/ITN917AI.url).

Patient Consent Statement

Subjects' consent was obtained according to the Declaration of Helsinki.

Permission to Reproduce

No materials from other sources are included in this manuscript.

Clinical Trial Registration

The subjects in this study were not enrolled in a clinical trial.

References

1. Higdon LE, Lee K, Tang Q, Maltzman JS. Virtual global transplant laboratory standard operating procedures for blood collection, PBMC isolation, and storage. Transplant Direct 2016, **2**, e101. doi:10.1097/TXD.0000000000000613
2. Fuss IJ, Kanof ME, Smith PD, Zola H. Isolation of whole mononuclear cells from peripheral blood and cord blood. Curr Protoc Immunol 2009, **Chapter 7**, 7.1.1–8. doi:10.1002/0471142735.im0701s85
3. Yi PC, Zhuo L, Lin J, Chang C, Goddard A, Yoon OK. Impact of delayed PBMC processing on functional and genomic assays. J Immunol Methods 2023, **519**, 113514. doi:10.1016/j.jim.2023.113514
4. Thyagarajan B, Barcelo H, Crimmins E, Weir D, Minnerath S, Vivek S, et al. Effect of delayed cell processing and cryopreservation on immunophenotyping in multicenter population studies. J Immunol Methods 2018, **463**, 61–70. doi:10.1016/j.jim.2018.09.007
5. Scheible K, Secor-Socha S, Wightman T, Wang H, Mariani TJ, Topham DJ, et al. Stability of T cell phenotype and functional assays following heparinized umbilical cord blood collection. Cytometry A 2012, **81**, 937–49. doi:10.1002/cyto.a.22203
6. Posevitz-Fejfár A, Posevitz V, Gross CC, Bhatia U, Kurth F, Schütte V, et al. Effects of blood transportation on human peripheral mononuclear cell yield, phenotype and function: implications for immune cell biobanking. PLoS One 2014, **9**, e115920. doi:10.1371/journal.pone.0115920
7. Palmirotta R, De Marchis ML, Ludovici G, Leone B, Savonarola A, Ialongo C, et al. Impact of preanalytical handling and timing for peripheral blood mononuclear cells isolation and RNA studies: the experience of the Interinstitutional Multidisciplinary BioBank (BioBIM). Int J Biol Markers 2012, **27**, e90–8. doi:10.5301/JBM.2012.9235
8. Olson WC, Smolkin ME, Farris EM, Fink RJ, Czarkowski AR, Fink JH, et al. Shipping blood to a central laboratory in multicenter clinical trials: effect of ambient temperature on specimen temperature, and effects of temperature on mononuclear cell yield, viability and immunologic function. J Transl Med 2011, **9**, 26. doi:10.1186/1479-5876-9-26
9. Navas A, Giraldo-Parra L, Prieto MD, Cabrera J, Gómez MA. Phenotypic and functional stability of leukocytes from human peripheral blood samples: considerations for the design of immunological studies. BMC Immunol 2019, **20**, 5. doi:10.1186/s12865-019-0286-z
10. Linggi B, Cremer J, Wang Z, Van Viegen T, Vermeire S, Lefevre P, et al. Effect of storage time on peripheral blood mononuclear cell isolation from blood collected in vacutainer CPT™ tubes. J Immunol Methods 2023, **519**, 113504. doi:10.1016/j.jim.2023.113504
11. Kobayashi DT, Decker D, Zaworski P, Klott K, McGonigal J, Ghazal N, et al. Evaluation of peripheral blood mononuclear cell processing and analysis for Survival Motor Neuron protein. PLoS One 2012, **7**, e50763. doi:10.1371/journal.pone.0050763
12. Johnson RK, Overlee BL, Sagen JA, Howe CL. Peripheral blood mononuclear cell phenotype and function are maintained after overnight shipping of whole blood. Sci Rep 2022, **12**, 19920. doi:10.1038/s41598-022-24550-6
13. Jerram A, Guy TV, Beutler L, Gunasegaran B, Sluyter R, Fazekas de St Groth B, et al. Effects of storage time and temperature on highly multiparametric flow analysis of peripheral blood samples; implications for clinical trial samples. Biosci Rep 2021, **41**, BSR20203827. doi:10.1042/BSR20203827
14. Hope CM, Huynh D, Wong YY, Oakey H, Perkins GB, Nguyen T, et al.; On Behalf Of The Endia Study Group. Optimization of blood handling and peripheral blood mononuclear cell cryopreservation of low cell number samples. Int J Mol Sci 2021, **22**, 9129. doi:10.3390/ijms22179129
15. Gottfried-Blackmore A, Rubin SJS, Bai L, Aluko S, Yang Y, Park W, et al. Effects of processing conditions on stability of immune analytes in human blood. Sci Rep 2020, **10**, 17328. doi:10.1038/s41598-020-74274-8
16. Golke T, Mucher P, Schmidt P, Radakovics A, Repl M, Hofer P, et al. Delays during PBMC isolation have a moderate effect on yield, but severly compromise cell viability. Clin Chem Lab Med 2022, **60**, 701–6. doi:10.1515/cclm-2022-0003
17. Bull M, Lee D, Stucky J, Chiu Y-L, Rubin A, Horton H, et al. Defining blood processing parameters for optimal detection of cryopreserved antigen-specific responses for HIV vaccine trials. J Immunol Methods 2007, **322**, 57–69. doi:10.1016/j.jim.2007.02.003
18. Betsou F, Gaignaux A, Ammerlaan W, Norris PJ, Stone M. Biospecimen science of blood for peripheral blood mononuclear Cell (PBMC) functional applications. Curr Pathobiol Rep 2019, **7**, 17–27. doi:10.1007/s40139-019-00192-8
19. Savage AK, Gutschow MV, Chiang T, Henderson K, Green R, Chaudhari M, et al. Multimodal analysis for human ex vivo studies shows extensive molecular changes from delays in blood processing. iScience 2021, **24**, 102404. doi:10.1016/j.isci.2021.102404
20. McKenna KC, Beatty KM, Vicetti Miguel R, Bilonick RA. Delayed processing of blood increases the frequency of activated CD11b+ CD15+ granulocytes which inhibit T cell function. J Immunol Methods 2009, **341**, 68–75. doi:10.1016/j.jim.2008.10.019
21. Bonilauri B, Santos MDM, Camillo-Andrade AC, Bispo S, Nogueira FCS, Carvalho PC, et al. The impact of blood-processing time on the proteome of human peripheral blood mononuclear cells. Biochim Biophys Acta Proteins Proteom 2021, **1869**, 140581. doi:10.1016/j.bbapap.2020.140581
22. Agashe C, Chiang D, Grishin A, Masilamani M, Jones SM, Wood RA, et al. Impact of granulocyte contamination on PBMC integrity of shipped blood samples: Implications for multi-center studies monitoring regulatory T cells. J Immunol Methods 2017, **449**, 23–7. doi:10.1016/j.jim.2017.06.004
23. Ji WJ, Lu RY, Liu JX, Ma Y-Q, Zeng S, Shi R, et al. The influence of different anticoagulants and time-delayed sample processing and measurements on human monocyte subset and monocyte-platelet aggregate analyses. Cytometry B Clin Cytom 2017, **92**, 371–9. doi:10.1002/cyto.b.21363
24. Wiedeman AE, Muir VS, Rosasco MG, DeBerg HA, Presnell S, Haas B, et al. Autoreactive CD8+ T cell exhaustion distinguishes subjects with slow type 1 diabetes progression. J Clin Invest 2020, **130**, 480–90. doi:10.1172/JCI126595
25. Patel AA, Zhang Y, Fullerton JN, Boelen L, Rongvaux A, Maini AA, et al. The fate and lifespan of human monocyte subsets in steady state and systemic inflammation. J Exp Med 2017, **214**, 1913–23. doi:10.1084/jem.20170355
26. Westera L, Drylewicz J, den Braber I, Mugwagwa T, van der Maas I, Kwast L, et al. Closing the gap between T-cell life span estimates from stable isotope-labeling studies in mice and humans. Blood 2013, **122**, 2205–12. doi:10.1182/blood-2013-03-488411

27. Marinova E, Han S, Zheng B. Human germinal center T cells are unique Th cells with high propensity for apoptosis induction. Int Immunol 2006, **18**, 1337–45. doi:10.1093/intimm/dxl066
28. Yap HY, Tee SZ, Wong MM, Chow S-K, Peh S-C, Teow S-Y. Pathogenic role of immune cells in rheumatoid arthritis: implications in clinical treatment and biomarker development. Cells 2018, **7**, 161. doi:10.3390/cells7100161
29. Listing J, Gerhold K, Zink A. The risk of infections associated with rheumatoid arthritis, with its comorbidity and treatment. Rheumatology 2013, **52**, 53–61. doi:10.1093/rheumatology/kes305
30. Weinberg A, Song L-Y, Wilkening C, Sevin A, Blais B, Louzao R, et al.; Pediatric ACTG Cryopreservation Working Group. Optimization and limitations of use of cryopreserved peripheral blood mononuclear cells for functional and phenotypic T-cell characterization. Clin Vaccine Immunol 2009, **16**, 1176–86. doi:10.1128/CVI.00342-08